# Histological and MS spectrometric analyses of the modified tissue of bulgy form tadpoles induced by salamander predation

**Tsukasa Mori[1,*], Yoichiro Kitani[1], Jun Ogihara[1], Manabu Sugiyama[1], Goshi Yamamoto[1], Osamu Kishida[2] and Kinya Nishimura[3]**

[1]Nihon University College of Bioresource Sciences, Kameino 1866, Fujisawa 252-0880, Japan
[2]Teshio Experimental Forest, Field Science Center for Northern Biosphere, Hokkaido University, Horonobe, Hokkaido, 098-2943, Japan
[3]Graduate School of Fisheries Sciences, Hokkaido University, Hakodate 041-8611, Japan
*Author for correspondence (mori.tsukasa@nihon-u.ac.jp)

*Biology Open* 000, 1–10
doi: 10.1242/bio2012604

## Summary

**The rapid induction of a defensive morphology by a prey species in face of a predation risk is an intriguing in ecological context; however, the physiological mechanisms that underlie this phenotypic plasticity remain uncertain. Here we investigated the phenotypic changes shown by *Rana pirica* tadpoles in response to a predation threat by larvae of the salamander *Hynobius retardatus*. One such response is the bulgy morph phenotype, a relatively rapid swelling in size by the tadpoles that begins within 4 days and reaches a maximum at 8 to 10 days. We found that although the total volume of bodily fluid increased significantly ($P<0.01$) in bulgy morph tadpoles, osmotic pressure was maintained at the same level as control tadpoles by a significant increase ($P<0.01$) in Na and Cl ion concentrations. In our previous report, we identified a novel frog gene named pirica that affects the waterproofing of the skin membrane in tadpoles. Our results support the hypothesis that predator-induced expression of pirica on the skin membrane causes retention of absorbed water. Midline sections of bulgy morph tadpoles showed the presence of swollen connective tissue beneath the skin that was sparsely composed of cells containing hyaluronic acid. Mass spectrographic (LC-MS/MS) analysis identified histone H3 and 14-3-3 zeta as the most abundant constituents in the liquid aspirated from the connective tissue of bulgy tadpoles. Immunohistochemistry using antibodies against these proteins showed the presence of non-chromatin associated histone H3 in the swollen connective tissue. Histones and 14-3-3 proteins are also involved in antimicrobial activity and secretion of antibacterial proteins, respectively. Bulgy tadpoles have a larger surface area than controls, and their skin often has bite wounds inflicted by the larval salamanders. Thus, formation of the bulgy morph may also require and be supported by activation of innate immune systems.**



Key words: Hyaluronic acid, LC-MS/MS, Histone H3, 14-3-3 zeta, Tadpole, Salamander

## Introduction

Phenotypic plasticity is the ability to produce different phenotypes under different environmental conditions and to respond to changes in environmental conditions. This phenomenon has long been studied by evolutionary biologists interested in its adaptive significance (Pigliucci, 2001; West-Eberhard, 2003). Inducible defenses, which involve phenotypic changes stimulated directly by cues associated with predation threat, are an example of phenotypic plasticity induced by a change in environmental conditions (Bronmark and Miner, 1992; Gilbert, 2009; Jarrett, 2009; Kishida and Nishimura, 2004; Tollrian, 1995; Tollrian and Harvell, 1999; Weisser et al., 1999). The morphological changes associated with predator-induced phenotypic plasticity involves a variety of physiological and anatomical systems, for example, the nervous system, metabolism, and connective tissues, among others. However, we have only a limited understanding of the mechanistic aspects of phenotypic plasticity in an ecological context (Piersma and Gils, 2011).

Predator-induced phenotypic plasticity of anuran tadpoles has been well studied in evolutionary ecology. Various species distributed in Asia, Europe and North America make a formation of a “high tail” in the presence of a predator threat (Kishida and Nishimura, 2005; McCollum and Leimberger, 1997; Van Buskirk et al., 1997). Among these, tadpoles of *Rana pirica*, also display another, unique morphology when exposed to their main predator, the larval salamander *Hynobius retardatus*; in this case the tadpoles form a “bulgy” morphology (Kishida and Nishimura, 2004). *R. pirica* tadpoles are presumed to have evolved the inducible bulgy morphology against the gape-limited *H. retardatus* larvae under an intimate predator-prey relationship (Kishida et al., 2007; Kishida et al., 2009; Michimae et al., 2005; Michimae and Wakahara, 2002). The bulgy morph is induced only by the predation threat of the larval salamanders and it functions to prevent the tadpoles from being swallowed (Kishida and Nishimura, 2004; Kishida and Nishimura, 2005). There is considerable interest in elucidating the underlying mechanisms of phenotypic plasticity in order to provide an integrated

understanding of physio-ecological phenomena (Crespi and Denver, 2005). The anuran tadpoles' morphological plasticity is also a useful system to study organism's physio-ecological response to external stress conditions.

We previously conducted a cDNA subtraction and microarray analyses of epithelial tissue from bulgy-morph and non-bulgy-morph tadpoles of *R. pirica* (Mori et al., 2005). We identified 13 down-regulated candidates and 19 up-regulated candidates. In the up-regulated group, 6 candidates were derived from the same gene, which was subsequently named pirica (Mori et al., 2009). Pirica encodes a protein similar to uromodulin or Tamm-Horsfall protein (THP). The protein has a zona pellucida domain; this domain in the C-terminal region of uromodulin enables polymerization into filaments (Jovine et al., 2002) and facilitates gel-forming mucoid capability (Serafini-Cessi et al., 2003). It has been suggested that the gel-forming capability of uromodulin within the thick ascending limb of Henle's loop (TALH) may contribute to the water permeability of the nephron (Kumar and Muchmore, 1990). An *in vitro* experiment using isolated uromodulin demonstrated that it could act as a water barrier but that it allowed ion movement (Mattey and Naftalin, 1992). Recently, an immunocytochemical study found that uromodulin was present in the kidney and skin of the frog *Rana temporaria* and that uromodulin-positive material was present in the distal renal tubules and nephric ducts of frogs, and in the superficial epidermis of the skin (Howie et al., 1991).

Expression of pirica genes in epithelium of the bulgy-morph tadpole appears to control the permeability of the superficial epidermis of the tadpole skin, suggesting that regulating the permeability of the skin might be important to water retention in the tadpole body.

We reached a deduction from our previous studies that evolution of the inducible bulgy morphology against the gape-limited *H. retardatus* larvae involved changes to the control of body water dynamics to attain the bulgy body that reduces predation risk. This conclusion leaves various questions unanswered, however. First, which tissues accumulate water to enable the rapid switch from normal to bulgy morph phenotype? Second, what changes occur in the affected tissues to allow them to accumulate water? Third, how does the tadpole prevent injury to the skin when expanding rapidly to the bulgy morph? With respect to the latter point, it is possible that the bulgy morph tadpole has a means to reduce infection risks to its expanded body.

To provide answers to these questions and thereby increase our understanding of predator-induced phenotypic plasticity, we performed a number of analyses: (1) we determined solute concentrations and osmotic pressures in the body fluids of bulgy morph compared to control tadpoles; (2) we investigated the location of the retained water during formation of the bulgy morph; (3) we performed a mass spectrophotometric (LC-MS/MS) analysis of the proteins present in the liquids forming the bulgy body; and (4) carried out an immunohistochemical analysis of the distribution of proteins shown by the LC-MS/MS analysis to be increased in bulgy morph tadpoles.

## Materials and Methods

### Preliminary experiment for samples preparation to investigate interaction of treatment and aquarium effects

Eggs of *R. pirica* and *H. retardatus* were collected from a pond in Hokkaido, Japan, and placed in 10-liter aquaria. After hatching, *R. pirica* tadpoles were fed rabbit chow ad libitum. The larval *H. retardatus* were fed small-sized *R. pirica* tadpoles ad libitum. Water in all aquaria was changed every second day. The experiment was conducted in a laboratory at 20℃, using a natural day/night (about 14/10 hours) regime. The experimental units were 2.5 liter aquaria (10 × 24 cm in surface area, and 10 cm in height) each filled with 2 liters of tap water filtered by activated charcoal. Thirty similarly sized 10-day-old tadpoles (about 18 mm) were randomly chosen from the holding tank, and were placed in each aquarium. The tadpoles were fed rabbit chow ad libitum daily, and the water of all aquaria was changed every second day throughout the experiment. The experiment consists of two treatments, predator-treatment (Ex aquarium 1–3) and control (C aquarium 1–3), respectively. Concerning predator-treatment, further two aquaria (Back aquarium 1, 2) were prepared for back up. The experiment was started when a larval salamander were introduced in predator-treatment aquarium. At two weeks, we sampled the tadpoles in the aquaria of each treatment.

During the experiment, to minimize unexpected predation of tadpoles in the predator-treatment aquarium, the salamander was replaced daily with another that had been kept in a holding tank containing sufficient *R. pirica* tadpoles to allow easy feeding. Replacement predators were randomly chosen from each holding tank. Every second day, we counted the tadpoles in each aquarium to check the number of survivors. If unexpected deaths reduced the number of tadpoles in an aquarium (Ex aquarium 1–3), we reallocated tadpoles from back up aquarium, which was chosen arbitrarily, to maintain a minimum of 30 tadpoles per aquarium in each treatment. Through such manipulation, we sought to eliminate any possible density effect on experimental results. In this experiment, we used tadpole weights as an indicator of bulgy morph formation. After two weeks, three randomly selected tadpoles from one aquarium were taken and weighed as a single sample after removal of residual water from the aquarium. Tadpole body weights were measured in triplicate using randomly selected tadpoles from the control and predator-treatment aquaria.

### Samples for histological and physiological analysis

Two groups of *Rana pirica* tadpoles, each containing approximately 1000 tadpoles, were maintained in 10 liter aquaria and fed rabbit chow ad libitum. Prior to the start of the experiment, larval *Hynobius retardatus* were fed small *R. pirica* tadpoles ad libitum. The water in the aquaria was changed every second day.

Two treatment groups were established: the predator-exposed group in which three salamanders were placed in one of the tanks of tadpoles for 2 weeks; and the control group that was not exposed to predators. The larval salamanders were regularly replaced to maintain a constant predation stress in the former treatment.

The experiment was conducted in a laboratory at 18℃, using a natural day/night regime (about 14/10 h). After two weeks of exposure to the predators, about 80% of the tadpoles fully displayed the induced bulgy form; at this date, bulgy tadpoles and controls were collected.

We selected tadpoles of approximately equal size from the bulgy morph group for histological and physiological analyses; similarly sized tadpoles were also chosen from the control group. In total, 51 bulgy morph and 50 control tadpoles were used in the analyses described here.

### Histological study

Tadpoles for histological study and immunohistochemistry were embedded in O.C.T. compound (Sakura) together with a centering marker to enable midline sections to be cut. The marker was prepared as follows: a piece of raw potato (*Solanum tuberosum*) was punched using a cork borer (ø 6.0 × 40.0 mm), and one end was sharpened to a taper (Fig. 1d–f). The marker was stained with iodine, embedded in O.C.T. compound in an aluminum foil trough, and then immediately frozen with dry-ice cooled n-hexane. The tadpole for sectioning was placed carefully over the marker (Fig. 1d–f), O.C.T. compound was carefully poured over, and then immediately frozen as above. Successfully frozen blocks were kept at -80℃ until used for sectioning. Sections were cut at a thickness of 4 µm using a CM1500 cryostat (Leica) and mounted on MAS coated glass microscope slides (Matsunami). By use of a centering marker, we can ensure that the analyzed sections are those of tadpoles cut across the midline. For example, if the section followed the line a to a' in Fig. 1g, then the centering marker would be cut along the line a to a' (Fig. 1h) and, therefore, clearly not along the midline. The resulting section of the tadpole would appear as in Fig. 1i. As is illustrated in the schematic diagrams in Fig. 1i-k, a successful midline section would resemble that shown in Fig. 1k. Using this sectioning strategy, we were able to ensure production of midline sections from bulgy and control tadpoles (Fig. 1l–o). For histological examination, the slides were stained with hematoxylin-eosin, Mallory-Azan, Fast-Red and alcian blue 8GS, as described elsewhere (Bancroft and Stevens, 1982). Measuring of the thickness in the connective tissue was also performed. The maximum thickness of the connective tissue from control (n=3) and bulgy (n=3) tadpoles were measured using the midline sections. The thickness was evaluated by using the Adobe Photoshop CS4 (Adobe systems). A line was drawn across the vertex of the connective tissue and the number of pixels that made up the length of the line was obtained from the software. The pixel number was transformed into a real length using the known number of pixels in a 500 µm line. Statistical analysis of the data was performed using Student's t-test, with $p<0.001$ being regarded as significant.

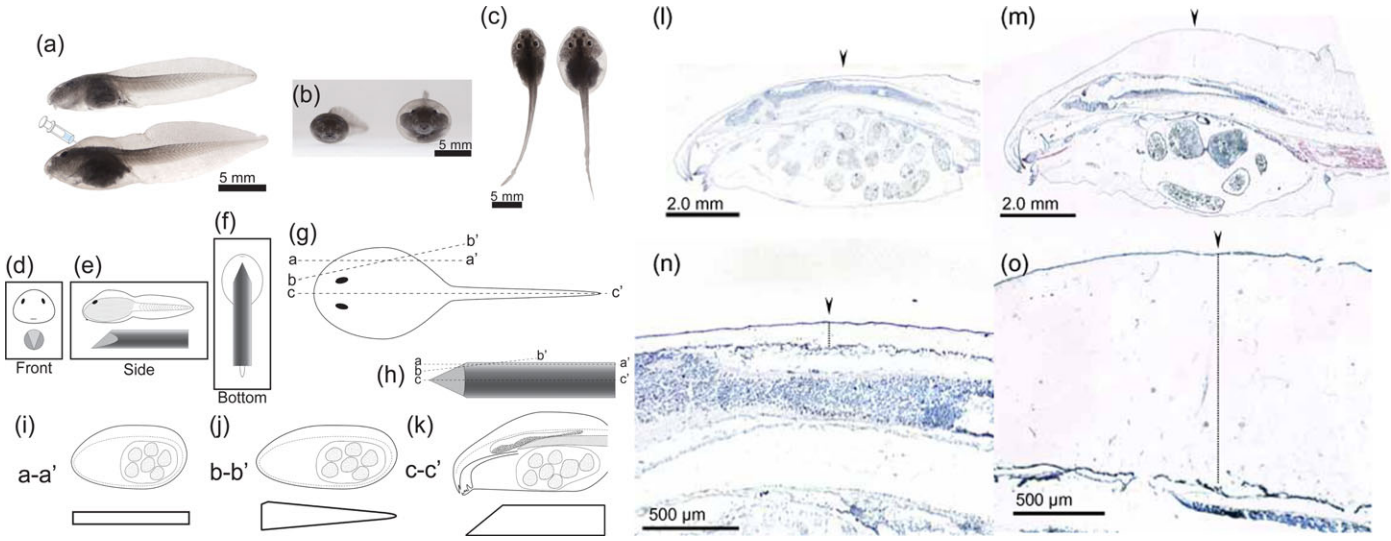


**Fig. 1. Comparative morphologies of control and the bulgy morph *R. pirica* tadpoles. (a–c)** Tadpoles are shown in side view (a), front view (b) and top view (c); the control tadpole is the upper specimen in (a) and the left specimen in (b) and (c), the bulgy morph tadpole is the lower specimen in (a) and the right specimen in (b) and (c). **(d–k)** Schematic diagrams illustrating the center marker method for ensuring preparation of midline sections. The tadpole is positioned over the midline of the center marker (d,e,f). (i) illustrates a section cut along the line a-a′ of the tadpole (g) and of the center marker (h). (j) illustrates an oblique section along the line b-b′ of the tadpole (g) and of the center marker (in h). (k) illustrates a midline section along the line e–f of the tadpole (g) and of the center marker (h). **(l–o)** Hematoxylin-eosin stained sections of control and bulgy morph tadpoles. Images of the head end of control (l) and bulgy morph (m) tadpoles, and their parietal regions (n, o, respectively).

In sections stained with Mallory-Azan, tissue with a high density of nuclei appeared red, while tissue with relatively low numbers of nuclei appeared blue. Positive alcian blue staining indicates the presence of acid mucus polysaccharides (Doliger et al., 1995; Sasai, 1971). To further characterize the swollen connective tissues of bulgy morph tadpoles, sections were treated with 1% alcian blue 8GS-1N HCl (pH 1.0, for strongly sulfated glycosaminoglycans) or 1% alcian blue 8GS-3% acetic acid (pH 2.5, for a broad range of acidic glycosaminoglycans).

Our mass spectrophotometric analyses (see below) indicated the possibility of hyaluronic acid accumulation in the tissues of bulgy morph tadpoles.

To confirm the presence of hyaluronic acid in connective tissues of the tadpoles, we pretreated sections with 40 units/ml hyaluronidase (from bovine testes, Nakarai Tesque, Kyoto, Japan) in PBS (pH 5.5) for 30 min at 37℃. After a brief wash with water, the sections were stained with alcian blue 8GX (pH 2.5) and Nuclear FastRed, as described above. The slides were screened using a conventional microscope.

## Measurements of body fluid, osmotic pressure and various ions

The tadpoles selected for analysis were placed on a Kimwipe tissue to remove any residual water from the aquarium, and then each tadpole was rapidly homogenized on ice for 30 seconds with a Polytron (Kinematica). The homogenized samples were centrifuged at 15,000 rpm for 30 min at 4℃. The volume of supernatant from each tadpole was measured using a micropipette; the supernatant was then used to determine osmotic pressure and Na, K, and Cl ion concentrations using an Osmometer (Asahilife Science) or a Dri-Chem 800, respectively.

Data from the bulgy morph tadpoles are expressed as values relative to those of controls.

## Sample preparation from bulgy morph tadpoles for LC-MS/MS analysis

Small amounts of liquid from the connective tissue of five bulgy tadpoles were obtained using an ultra fine needle without causing damage to the surrounding tissues. Crude protein extracts were prepared from 10 µl aliquots of the samples by boiling in SDS sample buffer (200 µl) for SDS-PAGE (62.5 mM Tris, 4% SDS, 25% glycerol, 0.002% bromophenol blue, and 5% β-mercaptoethanol, pH 6.8). The buffer plus sample was then centrifuged and the supernatant subjected to SDS-PAGE. The SDS-PAGE gel was stained by MS-compatible silver staining (Shevchenko et al., 1996). For the proteomic analysis, a single lane from the silver-stained gel was divided into 10 equal slices of 6 mm width. Each gel slice was cut into small pieces and put into a 1.5 ml tube. The gel pieces were destained by rinsing in destaining solution (15 mM $K_3[Fe(CN)_6]$, 50 mM $Na_2S_2O_3$). The disulfide bonds of cysteines were reduced by incubating with 10 mM dithiothreitol in 25 mM $NH_4HCO_3$ at 56℃ for 1 h and alkylated with 55 mM iodoacetamide in 25 mM $NH_4HCO_3$ at room temperature for 45 min in the dark. Gel pieces were washed with 50% acetonitrile and dried in a vacuum concentrator (CVE200D, Tokyo Rikakikai, Japan). The gel pieces were re-hydrated with 30 µl of trypsin solution (10 µg/ml in 50 mM $NH_4HCO_3$). In-gel digestion was performed at 37℃ during overnight and peptides were extracted with 50% acetonitrile containing 5% trifluoroacetic acid. Extracts were dried in a vacuum concentrator and re-dissolved in 0.1% (v/v) formic acid. The peptide mixtures were subjected to LC/MS and data-dependent tandem mass (LC/MS/MS) analyses.

## Mass spectrometric analysis

LC-MS/MS analysis was carried out in a LCQ Deca XP ion trap mass spectrometer (ThermoFinnigan, USA) equipped with a nano-LC electrospray ionization source (AMR, Japan), and interfaced on-line with a capillary HPLC system (Paradigm MS4, Michrom Bioresources, USA). Samples were introduced onto the analytical column using an autosampler (HTC-PAL system, CTC Analytics AG, Switzerland). Ten microliters of the peptide extract samples were first transferred onto a C8 cartridge (Peptide Captrap, Michrom Bioresources, USA) and the eluted peptides were then transferred onto the analytical column (L-column Micro C18, 0.2 mm × 50 mm, CERI, Japan) using a switching valve. Peptides were eluted using a gradient from buffer A (2% vol/vol acetonitrile, 0.1% formic acid) to buffer B (90% vol/vol acetonitrile, 0.1% formic acid).

Following an initial timed wash with buffer A, peptides were eluted using a linear gradient from 5–80% buffer B over a 30 min interval. The HPLC column eluent was eluted directly into the electrospray ionization source of an LCQ-Deca XP ion trap mass spectrometer.

Automated peak recognition, dynamic exclusion, and daughter ion scanning of the top two most intense ions were performed using the Xcalibur software as described previously (Andon et al., 2002; Haynes et al., 1998). Spectra were scanned over the range 450–2000 mass units.

## Database searching and data interpretation

MS/MS data were analyzed using SEQUEST (Bioworks v3.2, ThermoFisher, San Jose, CA), a computer program that allows the correlation of experimental data with theoretical spectra generated from known protein sequences (Eng et al., 1994; Yates et al., 1995). In this work, the criteria for a preliminary positive peptide identification of a doubly charged peptide were a correlation factor (Xcorr) greater than 2.5, a delta cross-correlation factor (deltaCn) greater than 0.1 (indicating a significant difference between the best match reported and the next best match), a high preliminary score, and a minimum of one tryptic peptide terminus. For triply charged peptides the correlation factor threshold was set at 3.5. All matched peptides were confirmed by visual examination of the spectra, and all spectra were searched against the latest version of the public non-redundant protein database of the National Center for Biotechnology Information (NCBI) (data were obtained from the nr.fasta data file of 2009, January /21). The data are summarized in Table 2 using the following abbreviations: P(pro) - probability of the best peptide match; Sf - the Sf score for

each peptide calculated by a neural network algorithm that incorporates Xcorr, DeltaCn, Sp, RSp, peptide mass, charge state, and the number of matched peptides for the search; Score - a value that is based upon the probability that the peptide is a random match to the spectral data; Coverage - the percent coverage based upon the amino acids of the protein; Peptide (Hits) - total number of peptide matches, and the number of proteins that were found to be related to that entry in parentheses.

### Immunohistochemistry

Following the results of the LC-MS/MS analysis, bulgy morph and non-bulgy tadpoles were subjected to immunohistochemical staining for histone H3 and 14-3-3 zeta.

Sections on slides were briefly rinsed with PBS and then soaked in blocking reagent, 2% gelatine in PBS, for 1 hour at 37℃. Next, the slides were incubated with a primary antibody for 1 hour at 37℃, either anti-pan 14-3-3 zeta antiserum (Enzo Life Sciences Inc. NY USA) diluted to 1/300 or anti-histone H3 polyclonal antibody (Santa Cruz Biotechnology, Inc. CA USA) diluted to 1/30. After a brief rinse in PBS containing 3% Tween 20 (PBST), the slides were incubated for 1 h at 37℃ with fluorescein isothiocyanate (FITC)-conjugated goat anti-rabbit IgG (Santa Cruz Biotechnology, Inc). As a negative control, we performed the staining with an anti-BSA antibody (home made) or no primary antibody. After washing with PBST, the sections were mounted with VECTASHIELD Mounting Medium with DAPI (Vector Laboratories, CA, USA), and the slides were observed using a BIOREVO BZ-9000fluorescence microscope (Keyence. Osaka, Japan). Double staining was performed using hematoxylin-eosin, and the slides were then analyzed with a conventional microscope.

## Results

### Theoretical aspects for sample preparation

We performed two different experiments for induction of bulgy formation in this report. The preliminary experiment was to observe the response of bulgy morph tadpoles exposed to salamanders and those not exposed to salamanders in different aquarium. The statistical model is given by

$$Y_{ijk} = \mu + \alpha_i + \beta_j + (\alpha\beta)_{ij} + \varepsilon_{ijk}\ (i = 1,2; j = 1,...,J; k = 1,...,K)$$

where $Y_{ijk}$ is the $(ijk)$th random variable corresponding to the response given by the $(ijk)$th bulgy morph tadpoles, $\mu$ is the overall population mean, $\alpha_i$ is the $i$th treatment effect, $\beta_j$ is the $j$th block effect corresponding to the $j$th aquarium, $(\alpha\beta)_{ij}$ is the $(ij)$th interaction effect between the $i$th treatment and $j$th block, and $\varepsilon_{ijk}$ is the $(ijk)$th random error. We emphasize that the number of bulgy morph tadpoles used in the experiment is $2JK$, i.e. $K$ is the number of replications within a same tank. The treatment is the stimulus given to the bulgy morph tadpoles, the levels of the treatment are either the presence or absence of salamanders in an aquarium. Three aquariums were used, i.e. $J = 3$, and the number of the bulgy morph tadpoles in each aquarium was 2 or 3, i.e. an unbalanced design was used. According to the analysis shown in Table 1, we will show that both the block effect $\beta_j$ and interaction effect of $(\alpha\beta)_{ij}$ will not be significant at 5% significant level. In other words, the reaction of the bulgy morph tadpoles exposed to or not exposed to the salamanders will not be influenced by placing them in a particular aquarium, i.e. we do not need to use different aquariums for further investigations. Therefore, the following new model is considered.

$$Y_{ik} = \mu + \alpha_i + \varepsilon_{ik}\ (i = 1,2; k = 1,...,K)$$

For consideration for the precision of the estimated mean effect due to the treatment, i.e. minimizing the variance of the estimated mean effect, the number of replications is increased considerably in the following experiment.

### Comparative histology of bulgy morph and control tadpoles

Based on an analysis of the results of a preliminary experiment, we decided that one control and one treated aquarium would be sufficient for the histological and physiological analyses.

Typical control and bulgy morph tadpoles obtained in this experiment are illustrated in Fig. 1a–c. We prepared midline sections of the tadpoles as shown in Fig. 1d–f in order to compare anatomical differences between the two phenotypes.

Analysis of midline sections showed drastic histological changes in the subdermal connective tissue of bulgy morph tadpoles (Fig. 1l–o). The connective tissue was obviously swollen in the bulgy morph tadpole and was more than 14.4 times thicker than in control tadpoles (Fig. 1n,o). The average thickness of the connective tissue in bulgy morph and control tadpoles was 1.2064 mm and 0.0839 mm, respectively. The difference in thickness between control and bulgy tadpoles was significant ($p<0.001$).

Furthermore, the swollen connective tissue was sparsely populated by cells compared to the control as we observed a relatively small number of hematoxylin stained nuclei. However, fibrous tissue that formed a network was present in the swollen connective tissue (Fig. 1o). The superficial epidermis and a small amount of connective tissue stained red with Mallory-Azan (Fig. 2a), whereas the connective tissue below the superficial epidermis and fibroblasts stained blue (Fig. 2a,b). Although the fibrous tissue that formed a network in swollen connective tissue was not stained by Mallory-Azan, a network in the parietal region showed clear staining with alcian blue (Fig. 3a). Further, altering the alcian blue stain from pH2.5 to pH1.0 resulted in the loss of the blue signal in the swollen connective tissue (compare Figs 3a,b) although a clear blue signal was still observed in cartilage at both pHs (Figs 3a,b). These results suggest the possibility that the target of the alcian blue in the swollen connective tissue was hyaluronic acid since only sulfate groups are stained by alcian blue at pH1.0 (Lev and Spicer, 1964). Support for this interpretation was received from the observation that the alcian blue signal in the swollen connective tissue disappeared after hyaluronidase treatment although a clear blue signal was still observed in cartilage (Fig. 3c).

**Table 1. Two-way ANOVA of the differences within and between aquaria holding control and predator exposed tadpoles.**
Exposure to predators caused a significant effect ($p<0.05$). However, variation between aquaria within each treatment group or due to the interaction term (between treatment groups and between aquaria) did not contribute significantly to the total variation.

| Source | df | Seq SS | Adj SS | Adj MS | F | P |
|---|---|---|---|---|---|---|
| Treatment | 1 | 0.38595 | 0.39251 | 0.39251 | 30.73 | 0.000 |
| Block | 2 | 0.00626 | 0.00626 | 0.00313 | 0.24 | 0.787 |
| Interaction between Treatment and block | 2 | 0.01019 | 0.01019 | 0.00509 | 0.40 | 0.681 |
| Error | 10 | 0.12774 | 0.12774 | 0.01277 | | |
| Total | 15 | 0.53013 | | | | |

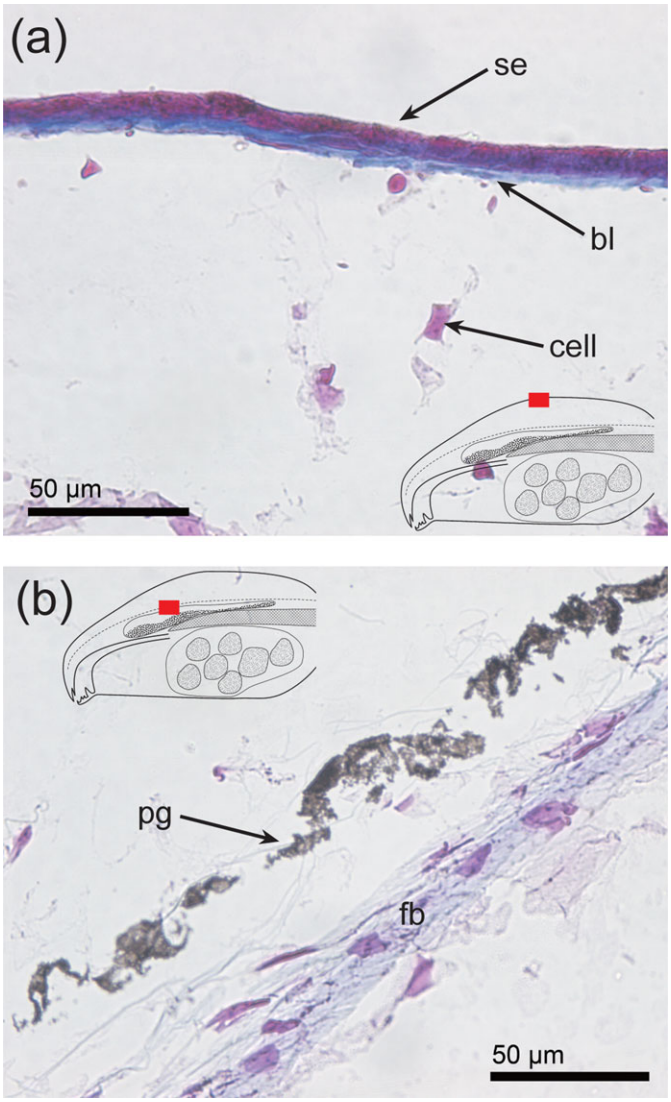


**Fig. 2. Sections through bulgy morph tadpoles.** The relative position of each image on the section is identified by the region highlighted in red in the superimposed line drawing. **(a,b)** Mallory-Azan staining of the parietal region. In (a), a typical region of the parietal surface is shown, while (b) shows the structure of a deeper part of the parietal region. bl, basal lamella; fb, fibroblast; cell, connective tissue cell; pg, pigment granule; se, squamous epithelium.

### Body fluid, osmotic pressure and various ions in the tadpoles

As water absorption is likely to be important for forming the bulgy shape, the total volume of fluid in bulgy morph and control tadpoles was measured (Fig. 4). Bulgy morph tadpoles had approximately 1.38 times more body fluid than control tadpoles, a difference that was significant ($P<0.01$). Generally, water absorption involves osmosis. We therefore compared osmotic pressures in bulgy morph and control tadpoles using the osmolarities of the fluids obtained from the tadpoles. We found no significant differences in the osmolarities of the extracted body fluids from bulgy morph and control tadpoles. This indicates that there must be differences in ionic absorption between bulgy morph and control tadpoles.

The absence of a difference in osmotic pressures between bulgy morph and control tadpoles, despite the significant difference in the total volume of body fluids, suggests the likelihood of differences in ion concentrations between the phenotypes (Fig. 5). We therefore measured the concentrations of ions that are important in determining the osmolarity of body fluid. The amounts of Na and Cl ions in the body fluid were approximately 1.8 times greater in bulgy morph than control tadpoles; these increase were significant ($p<0.01$). However, the two phenotypes did not show a significant difference ($p>0.05$) in the amount of K ions.

### Mass spectrometric analysis of the liquid materials from swollen connective tissue

Next, we attempted to analyze the constituents of the fluid in the bulgy morphs using LC-MS/MS. Although we were able to aspirate sufficient fluid from bulgy morph tadpoles using a fine needle (Fig. 1a), this was not feasible from control tadpoles as they did not have the engorged tissues seen in the bulgy morph. The fluid obtained from the bulgy morph tadpoles had the consistency of soft gel, possibly due to the presence of protein(s) or other compounds in the fluid.

A summary of the various peptides detected and identified is given in Table 2. Although the LC-MS/MS is not quantitative, proteins that are abundant are detected many times in the sample. On this basis, the most abundant peptides were histone H3 and 14-3-3 zeta (Table 2): histone and histone-related proteins were detected on 25 occasions, 14-3-3 zeta on 15 occasions, and actin and actin-related peptides on 12 occasions. Other peptides, such as SIPA1L1 protein, helicase DNA binding protein, amyloid beta, proteasome, ephrin receptor were also detected in the fluid from swollen connective tissue.

### Immunohistochemistry using anti-histone H3 and anti-14-3-3 zeta antibodies

Our LC-MS/MS analysis indicated that histone H3 and 14-3-3 zeta were the most common constituents of the fluid aspirated from the sparsely nucleated connective tissues of bulgy morph tadpoles. To investigate the distribution of these proteins further, we performed immunohistochemistry using anti-histone H3 and anti-14-3-3 zeta antibodies (Fig. 6). DAPI staining of nuclei was used to detect cells. As is clear from Figs 1 and 2, very few cells were observed in the swollen connective tissue. However, foci of anti-histone H3 antibody staining were present in both bulgy and control connective tissue (Fig. 6a–c, white arrows). These foci did not appear to be cell-like, and after HE staining they appeared as white circles (Fig. 6a). A strong signal was observed in the superficial epidermis of both bulgy and control tadpoles, and, interestingly, the signal was skewed towards the lower side of the superficial epidermis in the bulgy tadpole compared to the control (Fig. 6a,c). Our observations suggest that the histone H3 protein might be secreted from the superficial epidermis in the bulgy tadpole. Contrary to the results for histone H3, the anti-14-3-3 protein antibody localized to the superficial epidermis towards the top of the skin (Fig. 6d,f). Furthermore, the stained signals in foci or fibrous structures in the swollen connective tissue did not seem to be cellular in origin (Fig. 6d). However, in the bulgy morph but not control, a strong signal was also obtained in the deeper structure around the pigment granule of the parietal region (Fig. 6e). Negative controls using identical slides but no primary antibody had no signals (data not shown).

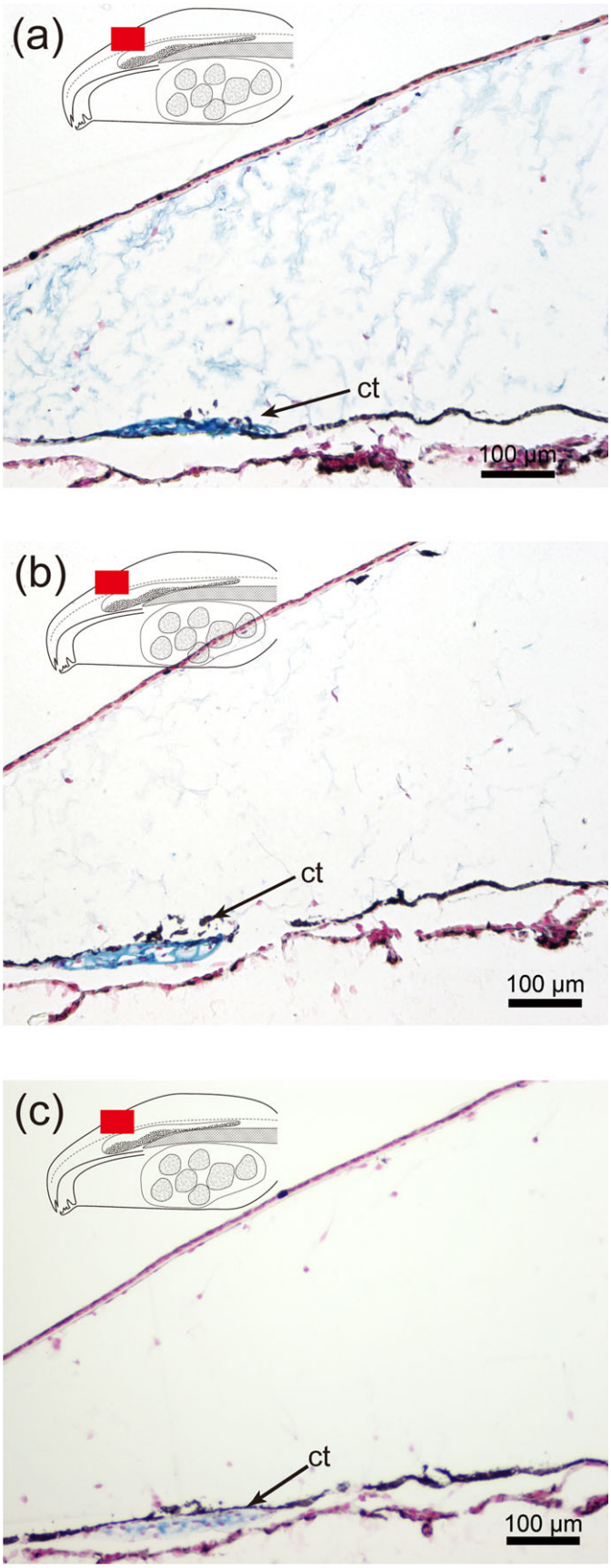


**Fig. 3. Sections through bulgy morph tadpoles and alcian blue staining of the parietal region. (a)** Section stained at pH2.5, **(b)** section stained at pH1.0, **(c)** section stained at pH2.5 after hyaluronidase treatment. Ct, cartilage.

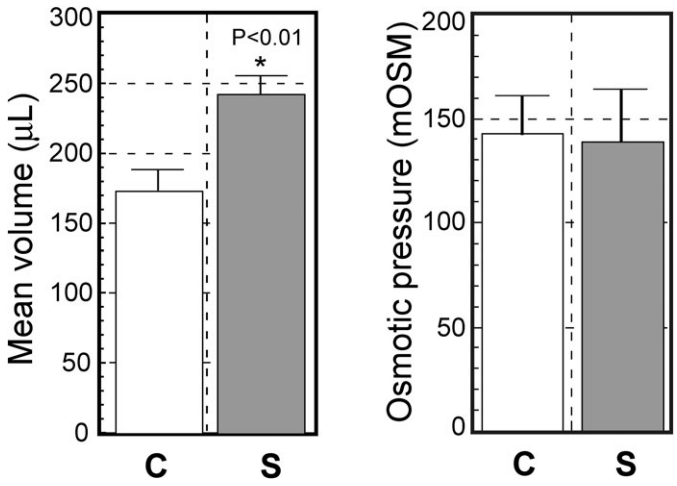


**Fig. 4. Effect of a predator on bodily fluid volumes and osmotic pressures in tadpoles.** Tadpoles were homogenized using a Polytron (Kinematica) and the homogenate centrifuged at 15,000 rpm for 30 min at 4℃. The total volume of supernatant from each tadpole was measured using a micropipette (n=24 control (C); n=25 bulgy morph (S) stimulated by predator); osmolarity was measured using the supernatant (n=14 control; n=15 bulgy morph). Vertical bars represent standard errors, and * indicates a significant difference by Student's t test ($p<0.01$).

## Discussion

Organisms have evolved a wide range of adaptive behaviors to avoid predation such as escape and hiding, changes in chemical composition, and morphological changes, among others. By forming a bulgy morph, *Rana pirica* tadpoles can reduce the risk of being swallowed by the gape-limited larval salamanders (Kishida and Nishimura, 2004; Kishida and Nishimura, 2005). The short-term solution of enlarging the body into a bulgy shape is more energy efficient than the long-term alternative of growing larger over a prolonged period, and the predation risk in the former is obviously lower than the latter. In our previous study, we identified the gene pirica, which has a 1296 bp open reading frame and translates into a putative 432 amino acid protein. The pirica protein is able to provide a waterproof layer because it has a zona pellucida domain that controls water permeation. In situ hybridization showed that the protein was up-regulated in the superficial epidermis (corresponding to the apical cells) of the bulgy morph (Mori et al., 2009). This finding suggested that formation of the bulgy phenotype is closely related to the retention of bodily fluids, resulting in the drastic thickening of the connective tissues (see Fig. 1).

The anuran larval epidermis consists of basal skin cells and apical cells (Robinson and Heintzelman, 1987; Utoh et al., 2000); a collagen lamella and connective tissue lie beneath the epidermis in the normal anuran tadpole (Utoh et al., 2000).

The osmoregulatory system appears to be important for bulgy morph formation. This system involves three organs, namely the gut, kidney and gills (similar to freshwater fish) in the tadpole. In adult frogs, four tissues are involved for osmoregulation, namely the gut, kidney, urinary bladder and skin. Generally, amphibian skin is freely permeable (Hillyard, 1999). Cutaneous permeability in adults frog results in substantial evaporative water loss when the animals are out of the water; this loss is compensated by water re-absorption through the nephron and the urinary bladder and, when the animals return to water, by uptake through the skin (Acher et al., 1997). This means that frog skin has high water

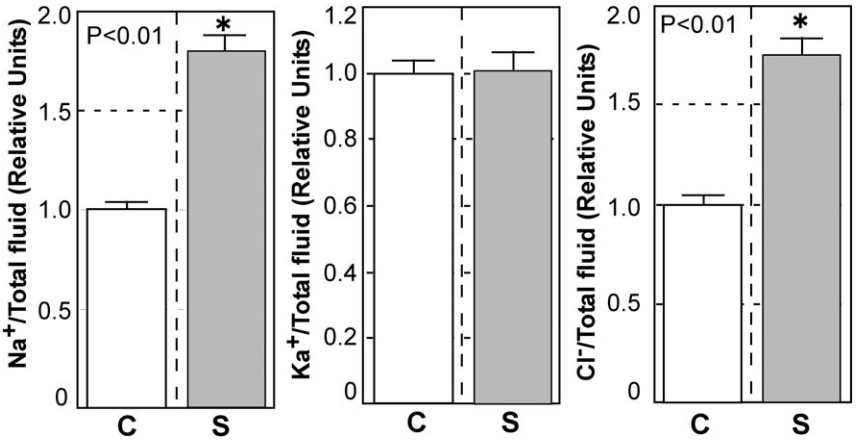


**Fig. 5. Changes in Na, K, and Cl ion concentrations in tadpoles exposed to a predator.** Tadpoles were homogenized using a Polytron (Kinematica) and the homogenate was centrifuged at 15,000 rpm for 30 min at 4℃. Na, K, Cl ion concentrations were measured in the supernatants of control (C) and bulgy morph (S) tadpoles (C, n=16; S, n=21); the data are expressed as values relative to control levels. Vertical bars represent standard errors, and * indicates a significant difference by Student's t test ($p<0.01$).

permeability. By comparison with adults, the skin of tadpoles has a simpler structure and is thinner.

As a consequence, the skin of a tadpole is water permeable, making water retention beneath the skin difficult. Therefore, formation of the bulgy shape in tadpoles may require alteration of the water permeability (i.e., a shutting down of water permeability) of the superficial epidermis of the skin, which might be achieved by expression of pirica (Mori et al., 2009).

Water retention in the tadpole body would thus use water re-absorbed through the nephron and the urinary bladder.

Our results (Figs 4, 5) suggested that water retention is an important factor in the formation of the bulgy morph phenotype. Additionally, our data indicated that the tadpoles maintained a constant osmotic pressure by increasing the concentration of Na and Cl ions in relation to the increase in water intake. Water retention and maintenance of a constant osmotic pressure in bulgy tadpoles resulted from pirica gene expression in the superficial epidermis of the skin, which changed from a water permeable into a waterproof layer.

The water that is retained in the bulgy morph is located in the connective tissue, which has a relatively sparse cell density that may make it easier to retain larger volumes of body fluids (Fig. 2a). In addition, hyaluronic acid in the connective tissue (Fig. 3c) plays an important role in the ground substance of higher vertebrates because of its water-binding quality (Elkan, 1976). Through this water-binding quality, the retained water becomes gel-like, leading to its stabilization in the bulgy form tadpole.

Hyaluronic acid is also known to be involved in the regulation of cell migration, proliferation and differentiation and in the activation of intercellular signaling cascades during tissue injury and repair (Jiang et al., 2007; Noble, 2002). The LC-MS/MS analysis of the gel-like material aspirated from the connective tissues of bulgy morph tadpoles showed that histone H3 and 14-3-3 zeta were the most common proteins present.

We were able to determine the immunohistochemical distributions of histone H3 and 14-3-3 zeta using commercially available antibodies (Fig. 6). Although these antibodies were prepared against human proteins, *R. pirica* histone H3 shows 95% sequence identity with its human homologue while 14-3-3 zeta shares 74% identity with its counterpart (GenBank:FS 289269.1). The signals obtained using these antibodies are therefore expected to provide an accurate description of the location of the target proteins.

Histones are small and abundant basic proteins that are most commonly found in association with DNA in the chromatin of eukaryotes. In addition to this role, there is also evidence that they have antimicrobial activity (Hiemstra et al., 1993). This property has been demonstrated for histone H2A and H2B in frog skin (Kawasaki et al., 2003) and skin mucosa of fish (Cho et al., 2002; Fernandes et al., 2002). It was reported that the histone family in various tissues display potential antibacterial functions, for example, histone H1 in fish skin (Fernandes et al., 2004) and H2B and H4 in the placenta (Ambrosio et al., 1997; Kim et al., 2002), and colon (Tollin et al., 2003).

The 14-3-3 genes encode a family of ubiquitous and highly conserved eukaryotic proteins, present in plants, fungi and animals. Although, this protein family comprises seven small molecules termed 14-3-3β, γ, ε, η, σ, τ, and ζ (zeta) (Hermeking, 2003; Hermeking and Benzinger, 2006), the most abundant of the 14-3-3 proteins identified by LC-MS/MS was 14-3-3zeta.

In animals, they are most abundant in the brain but are also present in a variety of other tissues (Boston et al., 1982). The proteins have numerous functions, and more than 100 binding partners have been identified in metabolic pathways for signal transduction, cell cycle regulation, apoptosis, stress responses, and malignant transformation (Darling et al., 2005).

14-3-3 proteins have been shown to be involved in exocytosis and signal transduction in many organisms. They can also bind to histones and affect both histone phosphorylation and dephosphorylation (Chen and Wagner, 1994), and can recognize a histone code on histone H3 (Winter et al., 2008). Analysis of histone H3 protein secretion from cultured sebocytes showed that 14-3-3 proteins are also present in secreted microvesicles (Nagai et al., 2005). The presence of 14-3-3 proteins in these sebocyte-derived vesicles suggests the proteins are involved in a novel cell function associated with the secretion of antibacterial proteins and in sterol regulation, and, thus, that they may play a crucial role in protecting the skin surface. These reports are highly relevant to our immunohistochemical results in which clear evidence of non-cellular histone proteins was obtained in the swollen connective tissue of bulgy tadpoles (Fig. 6a,b). Serial sections of bulgy tadpoles showed that the signal of the histone antibody was not associated with chromatin but indicated secreted protein. How else might secretion of H3 and 14-3-3 zeta benefit the bulgy morph tadpoles? Formation of the bulgy morph is relatively rapid and may place the skin under

**Table 2. Proteins identified in fluid aspirated from the swollen connective tissue of bulgy morph tadpoles.**

| Reference | Detected number | P (pro) | Sf | Score | Coverage | MW | Accession | Peptide (Hits) | Area (%) | Area Peak Area |
|---|---|---|---|---|---|---|---|---|---|---|
| Actin, gamma 1 propeptide | 2 | 4.04E-07 | 4.60 | 50.21 | 16.30 | 41792.6 | 4501887 | 5 (5 0 0 0 0) | 2.39 | |
| ACTB_XENBO | | 4.04E-07 | 4.60 | 50.21 | 16.20 | 41847.7 | 113271 | 5 (5 0 0 0 0) | 2.39 | |
| Actin, beta | | 4.04E-07 | 4.60 | 50.21 | 16.30 | 41752.5 | 47498068 | 5 (5 0 0 0 0) | 2.39 | |
| Actin, alpha 1, skeletal muscle | 4 | 4.04E-07 | 3.64 | 40.20 | 10.10 | 42015.7 | 148225448 | 4 (4 0 0 0 0) | 1.74 | |
| Similar to actin, alpha 1, skeletal muscle | | 4.04E-07 | 3.64 | 40.20 | 10.10 | 41983.6 | 147900780 | 4 (4 0 0 0 0) | 1.74 | |
| Smooth muscle alpha actin | | 4.04E-07 | 3.64 | 40.20 | 10.10 | 41905.7 | 62530438 | 4 (4 0 0 0 0) | 1.74 | |
| Actin, alpha 2, smooth muscle, aorta | | 4.04E-07 | 3.64 | 40.20 | 10.10 | 41977.7 | 58332196 | 4 (4 0 0 0 0) | 1.74 | |
| Xenopus laevis-like histone H3 | | 1.86E-02 | 1.99 | 40.12 | 9.60 | 15402.0 | 30268544 | 4 (4 0 0 0 0) | 1.06 | |
| Histone H3 | 11 | 1.86E-02 | 1.99 | 40.12 | 9.60 | 15373.9 | 148234575 | 4 (4 0 0 0 0) | 1.06 | |
| Histone cluster 1 | | 1.86E-02 | 1.99 | 40.12 | 9.60 | 15387.9 | 7305139 | 4 (4 0 0 0 0) | 1.06 | |
| Actin | | 4.04E-07 | 0.95 | 10.20 | 7.10 | 25234.5 | 37652183 | 1 (1 0 0 0 0) | 1.19 | |
| Histone H3a | | 1.54E-02 | 0.65 | 10.12 | 6.40 | 12195.1 | 90184624 | 1 (1 0 0 0 0) | 0.17 | |
| Histone cluster 1, H4a | | 1.03E-02 | 0.59 | 20.13 | 14.60 | 11367.3 | 4504301 | 2 (2 0 0 0 0) | 0.45 | |
| HIST1H2AH protein | | 6.84E-02 | 0.39 | 20.12 | 5.10 | 14758.8 | 71896475 | 4 (4 0 0 0 0) | 1.31 | |
| Cyclin D2 | | 1.00E+00 | 0.33 | 10.12 | 5.20 | 32959.2 | 148231416 | 1 (1 0 0 0 0) | 0.21 | |
| Histone H2B | | 1.00E+00 | 0.31 | 10.09 | 4.80 | 13905.1 | 122034 | 1 (1 0 0 0 0) | 0.06 | |
| Histone 2A | | 1.00E+00 | 0.31 | 10.08 | 4.90 | 13624.8 | 109157561 | 1 (1 0 0 0 0) | 0.06 | |
| Histone 1, H2bk | | 1.00E+00 | 0.31 | 10.08 | 4.80 | 13934.1 | 55742126 | 1 (1 0 0 0 0) | 0.06 | |
| Histone 2 | | 1.00E+00 | 0.31 | 10.08 | 4.80 | 13908.1 | 89273892 | 1 (1 0 0 0 0) | 0.06 | |
| Histone H2B | 3 | 1.00E+00 | 0.31 | 10.08 | 4.80 | 13841.9 | 296405 | 1 (1 0 0 0 0) | 0.06 | |
| SIPA1L1 protein | | 1.50E-03 | 0.29 | 10.10 | 0.90 | 196634.7 | 50604156 | 1 (1 0 0 0 0) | 0.08 | |
| 14-3-3 protein zeta | 15 | 1.00E+00 | 0.25 | 10.09 | 3.30 | 27875.9 | 71896217 | 2 (2 0 0 0 0) | 1.23 | |
| Histone H2A type 2 | | 1.00E+00 | 0.22 | 10.12 | 6.90 | 14000.2 | 1170158 | 3 (3 0 0 0 0) | 0.83 | |
| Chromodomain helicase DNA binding protein 4 | 2 | 1.00E+00 | 0.22 | 10.09 | 0.40 | 214685.8 | 148227774 | 1 (1 0 0 0 0) | 0.21 | |
| HLA-B associated transcript 2 | | 1.00E+00 | 0.20 | 10.09 | 0.40 | 223316.4 | 147906980 | 1 (1 0 0 0 0) | 0.25 | |
| Amyloid beta (A4) precursor protein-binding | | 1.00E+00 | 0.19 | 10.13 | 2.80 | 71055.5 | 147906548 | 1 (1 0 0 0 0) | 0.45 | |
| Histone H4 | | 1.00E+00 | 0.17 | 10.08 | 18.60 | 4915.8 | 50542195 | 1 (1 0 0 0 0) | 0.23 | |
| Proteasome (prosome, macropain) 26S subunit | | 4.65E-02 | 0.17 | 10.13 | 3.10 | 99274.0 | 62751452 | 1 (1 0 0 0 0) | 0.62 | |
| Ephrin receptor | 2 | 1.99E-02 | 0.13 | 10.08 | 0.80 | 109366.1 | 209969734 | 1 (1 0 0 0 0) | 0.50 | |

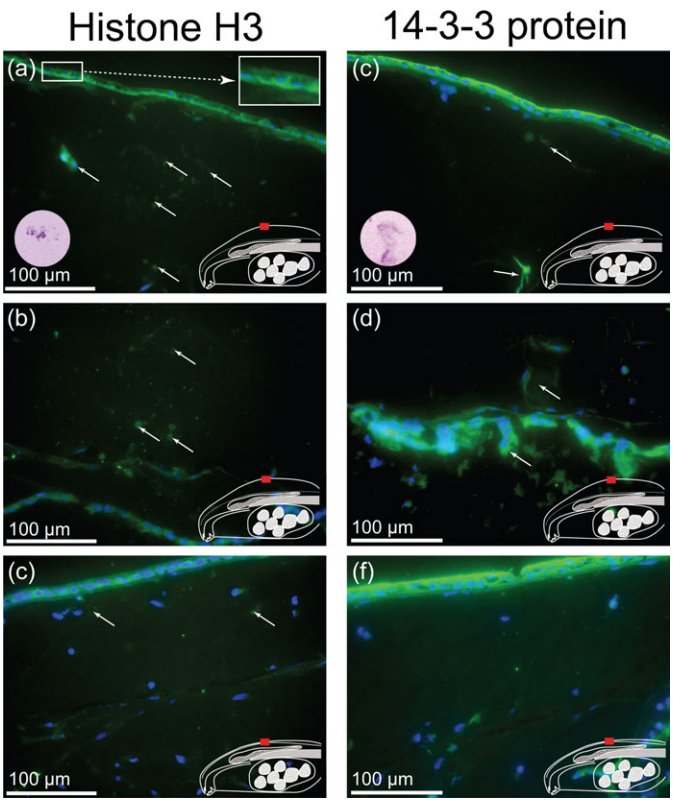


**Fig. 6. Immunohistochemical staining of midline sections.** Sections were incubated with anti-histone H3 antibody **(a,b,c)** or anti-14-3-3 zeta antibody **(d,e,f)**. (a,d) Parietal surface of bulgy morph tadpole. (b,e) Deeper structures of the parietal region of the bulgy morph tadpole. (c,f) Surface and deeper structure of parietal region of control tadpoles. Arrows indicate stained proteins, the superimposed circular images show HE staining of material stained by each antibody.

stress: the surface area of the bulgy morph tadpole is up to twice as large as that of controls. Moreover, bulgy tadpoles often have bite wounds resulting from attempted predation by the larval salamanders. These factors may increase the risk of infection in the bulgy morph tadpoles. Secretion of histone H3 with hyaluronic acid, stimulated by 14-3-3 zeta, may provide some measure of antimicrobial protection to the tadpoles. Thus, formation of the bulgy morph to reduce predation risk involves a clear remodeling of the connective tissues and physiological control of bodily fluids, and may also be supported by activation of innate immune systems.

As is shown in Fig. 1a, the bulgy form results from extreme changes to the connective tissue. 14-3-3 zeta was secreted from the skin and in the deeper structures of the parietal region of bulgy tadpoles (Fig. 6), and interacted with histone H3. Therefore, 14-3-3 zeta might play a role in the secretion of histone H3, and the drastic differences in expression of 14-3-3 zeta in the deeper structures of the parietal region of bulgy compared to control tadpoles (Fig. 6e,f) might be indicative of important events in bulgy morph formation.

## Acknowledgements

This work was funded in part by High Tech Research for private schools of Japan and by grants from the Japanese Educational Ministry (16657071), and Nihon University Multidisciplinary Research Grant for 2007 to MT. MT also deeply appreciated Dr Yukio Yanagisawa for his help and advice for manuscript preparation.

## Competing Interests

The authors declare no competing interests.

## References

**Acher, R., Chauvet, J. and Rouille, Y.** (1997). Adaptive evolution of water homeostasis regulation in amphibians: vasotocin and hydrins. *Biol. Cell* **89**, 283-291.

**Ambrosio, A. L., Iglesias, M. M. and Wolfenstein-Todel, C.** (1997). The heparin-binding lectin from ovine placenta: purification and identification as histone H4. *Glycoconjugate J.* **14**, 831-836.

**Andon, N. L., Hollingworth, S., Koller, A., Greenland, A. J., Yates, J. R., III and Haynes, P. A.** (2002). Proteomic characterization of wheat amyloplasts using identification of proteins by tandem mass spectrometry. *Proteomics* **2**, 1156-1168.

**Bancroft, J. D. and Stevens, A.** (1982). *Theory And Practice Of Histological Techniques*. NewYork: Churchill Livingstone.

**Boston, P. F., Jackson, P. and Thompson, R. J.** (1982). Human 14-3-3 protein: radioimmunoassay, tissue distribution, and cerebrospinal fluid levels in patients with neurological disorders. *J. Neurochem.* **38**, 1475-1482.

**Bronmark, C. and Miner, J. G.** (1992). Predator-Induced Phenotypical Change in Body Morphology in Crucian Carp. *Science* **258**, 1348-1350.

**Chen, F. and Wagner, P. D.** (1994). 14-3-3 proteins bind to histone and affect both histone phosphorylation and dephosphorylation. *FEBS Lett.* **347**, 128-132.

**Cho, J. H., Park, I. Y., Kim, H. S., Lee, W. T., Kim, M. S. and Kim, S. C.** (2002). Cathepsin D produces antimicrobial peptide parasin I from histone H2A in the skin mucosa of fish. *FASEB J.* **16**, 429-431.

**Crespi, E. J. and Denver, R. J.** (2005). Ancient origins of human developmental plasticity. *Am. J. Hum. Biol.* **17**, 44-54.

**Darling, D. L., Yingling, J. and Wynshaw-Boris, A.** (2005). Role of 14-3-3 proteins in eukaryotic signaling and development. *Curr. Top. Dev. Biol.* **68**, 281-315.

**Doliger, S., Delverdier, M., More, J., Longeart, L., Regnier, A. and Magnol, J. P.** (1995). Histochemical study of cutaneous mucins in hypothyroid dogs. *Vet. Pathol.* **32**, 628-634.

**Elkan, E.** (1976). *Ground substance: an anuran defense agent against desiccation.* New York: London Academic Press.

**Eng, J. K., McCormack, A. L. and Yates, J. R., III**. (1994). An approach to correlate tandem mass spectral data of peptides with amino acid sequences in a protein database. *J. Am. Soc. Mass Spectrom.* **5**, 976-989.

**Fernandes, J. M., Kemp, G. D., Molle, M. G. and Smith, V. J.** (2002). Anti-microbial properties of histone H2A from skin secretions of rainbow trout, Oncorhynchus mykiss. *Biochem. J.* **368**, 611-620.

**Fernandes, J. M., Molle, G., Kemp, G. D. and Smith, V. J.** (2004). Isolation and characterisation of oncorhyncin II, a histone H1-derived antimicrobial peptide from skin secretions of rainbow trout, Oncorhynchus mykiss. *Dev. Comp. Immunol.* **28**, 127-138.

**Gilbert, J. J.** (2009). Predator-specific inducible defenses in the rotifer Keratella tropica. *Freshw. Biol.* **54**, 1933-1946.

**Haynes, P. A., Fripp, N. and Aebersold, R.** (1998). Identification of gel-separated proteins by liquid chromatography-electrospray tandem mass spectrometry: comparison of methods and their limitations. *Electrophoresis* **19**, 939-945.

**Hermeking, H.** (2003). The 14-3-3 cancer connection. *Nat. Rev. Cancer* **3**, 931-943.

**Hermeking, H. and Benzinger, A.** (2006). 14-3-3 proteins in cell cycle regulation. *Semin. Cancer Biol.* **16**, 183-192.

**Hiemstra, P. S., Eisenhauer, P. B., Harwig, S. S., van den Barselaar, M. T., van Furth, R. and Lehrer, R. I.** (1993). Antimicrobial proteins of murine macrophages. *Infect. Immun.* **61**, 3038-3046.

**Hillyard, S. D.** (1999). Behavioral, molecular and integrative mechanisms of amphibian osmoregulation. *J. Exp. Zool.* **283**, 662-674.

**Howie, A. J., Lote, C. J. and Hillis, A. N.** (1991). Immunoreactive Tamm-Horsfall protein in the kidney and skin of the frog Rana temporaria. *Cell Tissue Res.* **263**, 585-587.

**Jarrett, J. N.** (2009). Predator-Induced Defense in the Barnacle Chthamalus Fissus. *J. Crustacean Biol.* **29**, 329-333.

**Jiang, D., Liang, J. and Noble, P. W.** (2007). Hyaluronan in tissue injury and repair. *Annu. Rev. Cell Dev. Biol.* **23**, 435-461.

**Jovine, L., Qi, H., Williams, Z., Litscher, E. and Wassarman, P. M.** (2002). The ZP domain is a conserved module for polymerization of extracellular proteins. *Nat. Cell Biol.* **4**, 457-461.

**Kawasaki, H., Isaacson, T., Iwamuro, S. and Conlon, J. M.** (2003). A protein with antimicrobial activity in the skin of Schlegel's green tree frog Rhacophorus schlegelii (Rhacophoridae) identified as histone H2B. *Biochem. Biophys. Res. Commun.* **312**, 1082-1086.

**Kim, H. S., Cho, J. H., Park, H. W., Yoon, H., Kim, M. S. and Kim, S. C.** (2002). Endotoxin-neutralizing antimicrobial proteins of the human placenta. *J. Immunol.* **168**, 2356-2364.

**Kishida, O. and Nishimura, K.** (2004). Bulgy tadpoles: inducible defense morph. *Oecologia* **140**, 414-421.

**Kishida, O. and Nishimura, K.** (2005). Multiple inducible defences against multiple predators in the anuran tadpole, Rana pirica. *Evol. Ecol. Res.* **7**, 619-631.

**Kishida, O., Trussell, G. C. and Nishimura, K.** (2007). Geographic variation in a predator-induced defense and its genetic basis. *Ecology* **88**, 1948-1954.
**Kishida, O., Trussell, G. C., Nishimura, K. and Ohgushi, T.** (2009). Inducible defenses in prey intensify predator cannibalism. *Ecology* **90**, 3150-3158.
**Kumar, S. and Muchmore, A.** (1990). Tamm-Horsfall protein--uromodulin (1950-1990). *Kidney Int.* **37**, 1395-1401.
**Lev, R. and Spicer, S. S.** (1964). Specific Staining Of Sulphate Groups With Alcian Blue At Low Ph. *J. Histochem. Cytochem.* **12**, 309.
**Mattey, M. and Naftalin, L.** (1992). Mechanoelectrical transduction, ion movement and water stasis in uromodulin. *Experientia* **48**, 975-980.
**McCollum, S. A. and Leimberger, J. D.** (1997). Predator-induced morphological changes in an amphibian: Predation by dragonflies affects tadpole shape and color. *Oecologia* **109**, 615-621.
**Michimae, H. and Wakahara, M.** (2002). A tadpole-induced polyphenism in the salamander Hynobius retardatus. *Evolution* **56**, 2029-2038.
**Michimae, H., Nishimura, K. and Wakahara, M.** (2005). Mechanical vibrations from tadpoles' flapping tails transform salamander's carnivorous morphology. *Biol. Lett.* **1**, 75-77.
**Mori, T., Hiraka, I., Kurata, Y., Kawachi, H., Kishida, O. and Nishimura, K.** (2005). Genetic basis of phenotypic plasticity for predator-induced morphological defenses in anuran tadpole, Rana pirica, using cDNA subtraction and microarray analysis. *Biochem. Biophys. Res. Comm.* **330**, 1138-1145.
**Mori, T., Kawachi, H., Imai, C., Sugiyama, M., Kurata, Y., Kishida, O. and Nishimura, K.** (2009). Identification of a novel uromodulin-like gene related to predator-induced bulgy morph in anuran tadpoles by functional microarray analysis. *PLoS ONE* **4**, e5936.
**Nagai, A., Sato, T., Akimoto, N., Ito, A. and Sumida, M.** (2005). Isolation and identification of histone H3 protein enriched in microvesicles secreted from cultured sebocytes. *Endocrinology* **146**, 2593-2601.
**Noble, P. W.** (2002). Hyaluronan and its catabolic products in tissue injury and repair. *Matrix Biol.* **21**, 25-29.
**Piersma, T. and Gils, J. A. V.** (2011). *The Flexible Phenotype: A Body-Centered Integration Of Ecology, Physiology, And Behaviour*. Oxford: Oxford University Press.
**Pigliucci, M.** (2001). *Phenotypic Plasticity: Beyond Nature And Nurture*. Baltimore: Johns Hopkins University Press.
**Robinson, D. H. and Heintzelman, M. B.** (1987). Morphology of ventral epidermis of Rana catesbeiana during metamorphosis. *Anat. Rec.* **217**, 305-317.
**Sasai, Y.** (1971). Identification of individual acid mucopolysaccharide in tissue sections. *Tohoku J. Exp. Med.* **105**, 101-110.
**Serafini-Cessi, F., Malagolini, N. and Cavallone, D.** (2003). Tamm-Horsfall glycoprotein: biology and clinical relevance. *Am. J. Kidney Dis.* **42**, 658-676.
**Shevchenko, A., Wilm, M., Vorm, O. and Mann, M.** (1996). Mass spectrometric sequencing of proteins silver-stained polyacrylamide gels. *Anal. Chem.* **68**, 850-858.
**Tollin, M., Bergman, P., Svenberg, T., Jornvall, H., Gudmundsson, G. H. and Agerberth, B.** (2003). Antimicrobial peptides in the first line defence of human colon mucosa. *Peptides* **24**, 523-530.
**Tollrian, R.** (1995). Predator-Induced Morphological Defenses - Costs, Life-History Shifts, and Maternal Effects in Daphnia-Pulex. *Ecology* **76**, 1691-1705.
**Tollrian, R. and Harvell, C. D.** (1999). *The ecology and evolution of inducible defenses.* Princeton, NJ: Princeton University Press.
**Utoh, R., Asahina, K., Suzuki, K., Kotani, K., Obara, M. and Yoshizato, K.** (2000). Developmentally and regionally regulated participation of epidermal cells in the formation of collagen lamella of anuran tadpole skin. *Dev. Growth Differ.* **42**, 571-580.
**Van Buskirk, J., McCollum, S. A. and Werner, E. E.** (1997). Natural selection for environmentally induced phenotypes in tadpoles. *Evolution* **51**, 1983-1992.
**Weisser, W. W., Braendle, C. and Minoretti, N.** (1999). Predator-induced morphological shift in the pea aphid. *Proc. R. Soc. London Ser. B* **266**, 1175-1181.
**West-Eberhard, M. J.** (2003). *Developmental plasticity and evolution.* Oxford: Oxford University Press.
**Winter, S., Simboeck, E., Fischle, W., Zupkovitz, G., Dohnal, I., Mechtler, K., Ammerer, G. and Seiser, C.** (2008). 14-3-3 proteins recognize a histone code at histone H3 and are required for transcriptional activation. *EMBO J.* **27**, 88-99.
**Yates, J. R., III, Eng, J. K., McCormack, A. L. and Schieltz, D.** (1995). Method to correlate tandem mass spectra of modified peptides to amino acid sequences in the protein database. *Anal. Chem.* **67**, 1426-1436.